

## Applicability of Numerical Simulation by Particle Method to Unconfined Compression Tests on Geomaterials

Sudip Shakya<sup>1</sup> , Shinya Inazumi<sup>2\*</sup> 

<sup>1</sup> Graduate School of Engineering and Science, Shibaura Institute of Technology, Koto-ku, Tokyo 135-8548, Japan.

<sup>2</sup> College of Engineering, Shibaura Institute of Technology, Koto-ku, Tokyo 135-8548, Japan.

Received 31 October 2023; Revised 11 December 2023; Accepted 21 December 2023; Published 01 January 2024

### Abstract

This study emphasizes the importance of accurate input parameters for ensuring the precision and reliability of simulations by conducting a sensitivity analysis to determine the calculation and material parameters. The aim is to determine the exact material parameters, for two different soil samples in a rigid state, by comparing the results of a sensitivity analysis with the unconfined compression test benchmark data for each sample. The moving particle semi-implicit (MPS) method, one of the particle methods, was chosen to reproduce the unconfined compression test simulation. The soil particles were assumed to be in the rigid state of the Bingham fluid bi-viscosity model. The first part of the study focuses on a sensitivity analysis of the basic simulation parameter values inputted during the simulation setup for the calculation procedure and the selection of the criteria for the calculation method, and then recommends the optimum values for a higher degree of accuracy based on the results. The second part of the study uses the results to analyze the sensitivity of each influencing parameter of the bi-viscosity Bingham fluid. In the final section, this study will provide a general guideline for selecting the optimum values for the MPS parameters and will recommend approximate values for other soil samples in future research with properties similar to those used in this study.

*Keywords:* Bi-viscosity Model; Geomaterial; Particle Method, Sensitivity Analysis; Unconfined Compression Test.

### 1. Introduction

In the field of geotechnical engineering, soil particles are assumed to be a viscous fluid, defined by their viscosity-related features during a numerical simulation by the particle method [1–4]. This also applies to soil with varying physical and mechanical properties [4, 5], resulting from the influence of the initial water content [6–8]. It is widely accepted that liquefied soil be represented by the Bingham fluid in simulations [9–13] because the Bingham fluid is mainly defined by the yield stress and viscosity [14, 15]. However, the analysis becomes impossible when the Bingham fluid is in a rigid state in which the shear stress does not exceed the yield stress [16, 17]. Meanwhile, the Bingham fluid bi-viscosity model defines the dual nature of the soil, assuming it to be a viscous-plastic fluid in a fluid state and a highly viscous fluid in a rigid state [18, 19]. Regardless of the soil state, soil can be represented in simulations by Bingham fluid [4, 5].

The precision of a simulation depends on the correct rheology and may require the use of the modified Bingham fluid model to explain the complex rheological behavior [20, 21]. Soil is comparable to concrete or mortar in terms of its flowability, and thus, the flowability values of these materials are often used as a reference when determining the plastic viscosity value [22, 23]. Aierken et al. [22] explained the compatibility of bi-viscosity Bingham fluid in a mortar flow simulation. Shakya et al. [23] suggested the extrapolation of the flow value vs. plastic viscosity, and the plastic

\* Corresponding author: [inazumi@shibaura-it.ac.jp](mailto:inazumi@shibaura-it.ac.jp)

 <http://dx.doi.org/10.28991/CEJ-2024-010-01-01>



© 2024 by the authors. Licensee C.E.J, Tehran, Iran. This article is an open access article distributed under the terms and conditions of the Creative Commons Attribution (CC-BY) license (<http://creativecommons.org/licenses/by/4.0/>).

viscosity value is obtained when the flow value is zero. However, both studies assume the flow behavior of the soil, and neither addresses the rigid state of the soil. Shakya et al. [22] suggested the recreation of unconfined compression tests to determine the material parameters because these tests are the simplest tests available for reproducing the widely used data in geotechnical engineering [24, 25]. Shakya et al. [14] conducted a sensitivity analysis for the particle size through an unconfined compression test simulation. Meanwhile, Shakya et al. [26] established a general thumb rule for yield parameter value selection criteria as well as the relationship between the yield value and plastic viscosity. However, their study was conducted for a yield value input equivalent to the unconfined compressive strength, and the yield value is generally taken as half of the unconfined compressive strength [8, 27]. Furthermore, the interrelation between the parameters under the influence of the remaining parameters has not yet been explored, nor has a reliable rationale for choosing a calculation method been addressed. Hence, there is a need to create an appropriate guideline that outlines a procedure for conducting sensitivity analyses of all relative parameters for the sake of more highly accurate simulation results.

This study will utilize the moving particle semi-implicit (MPS) method to establish a sensitivity analysis for the influencing parameters of the Bingham fluid bi-viscosity model. An attempt will be made to reproduce the realistic uniaxial compression test results that best fit the stress-strain relationship of the test samples and infer the actual material parameter values by comparing the inputted analysis values that generate the optimum results. The first section examines the parameters related to the mode of calculation, such as the interparticle distance, initial time interval, and radius of influence of the particles. The second section studies a sensitivity analysis for the plastic viscosity, critical shear strain, and yield value.

## 2. Material and Methods

### 2.1. Unconfined Compression Test Data

The unconfined compression test (UCT) has been extensively used in geotechnical engineering to determine the compressive strength and shear strength parameters, like cohesion and the angle of friction of cohesive soil, under unconfined conditions. It is also used to assess the mechanical properties of soil and to provide the stress-strain characteristics of soil. Depending upon the objectives of the study, UCTs can be conducted on undisturbed, reconstituted, or compacted cohesive soil samples. The results of UCTs on compacted samples are useful for evaluating the stability and load-bearing capacity of infrastructure. Meanwhile, reconstituted soil samples are useful for studying the intrinsic soil properties, such that a benchmark can be established for making comparisons with different soil samples. However, undisturbed samples are useful for accessing the behavior of a soil in its natural state, such as its natural cohesion, angle of friction, and stress-strain behavior. This information is crucial for accurate geotechnical designs and analyses.

Table 1 shows the soil properties of the two undisturbed samples utilized in this study. They are classified as clay and sand, respectively, according to the United States Department of Agriculture's (USDA) soil classification. The table includes details like the particle size distribution of the sample specimens and other soil properties, such as water content, unconfined compressive strength, etc., along with the actual dimensions of the samples that were extracted from the field for the experiment. The clay and sand samples are referred to as Sample 1 and Sample 2, respectively. Figure 1 shows the soil particle distribution curve for Sample 1. Figure 2 shows the experimental stress-strain characteristics of the two samples used in this study when the strain rate of 1% per minute is applied.

**Table 1. Particle size distribution and soil properties of Samples 1 and 2**

Sample name	Sample 1	Sample 2	
Soil classification	Clay	Sand	
Bulk density(g/cm <sup>3</sup> )	1.667	1.838	
Particle size distribution	0.075 – 2 mm (%)	20	92.4
	0.005 – 0.075 mm (%)	38	4.4
	< 0.005 mm (%)	42	3.2
	D <sub>60</sub> (mm)	0.020	NA
	D <sub>50</sub> (mm)	0.010	NA
	D <sub>30</sub> (mm)	-	NA
	D <sub>10</sub> (mm)	-	NA
	Max. soil size (mm)	2	0.85
Consistency properties	Liquid limit w <sub>L</sub> (%)	64.0	NA
	Plastic limit w <sub>P</sub> (%)	28.6	NA
	Plasticity index I <sub>P</sub>	35.4	NA

Sample condition	Undisturbed	Undisturbed
Water content (%)	53.7	22.5
Unconfined compressive strength (kN/m <sup>2</sup> )	25.8	39.5
Failure strain (%)	0.7	1.48
Dimensions	5*10 cm	5.02*9.82 cm

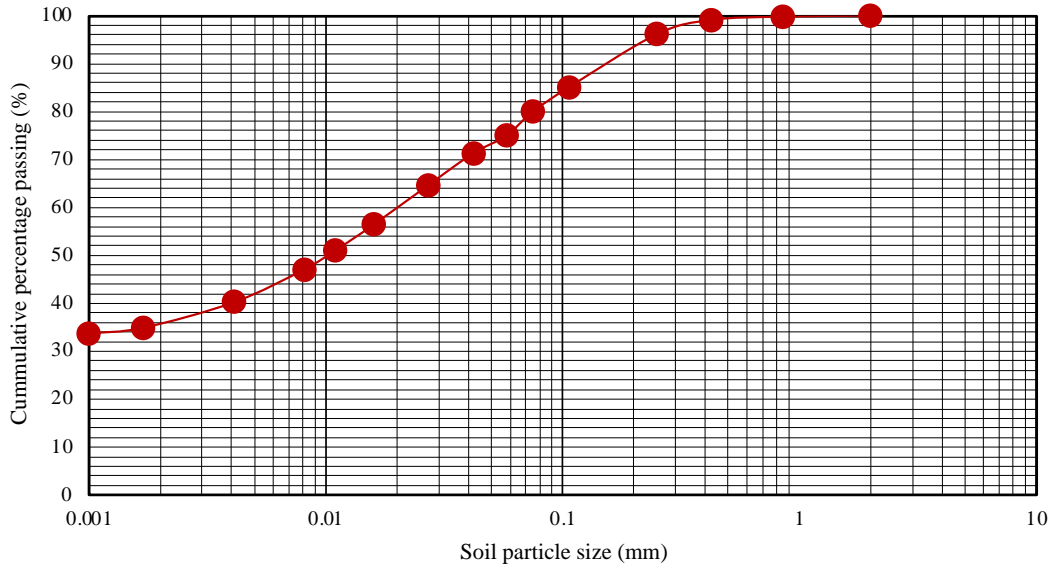


Figure 1. Soil particle distribution curve for Sample 1

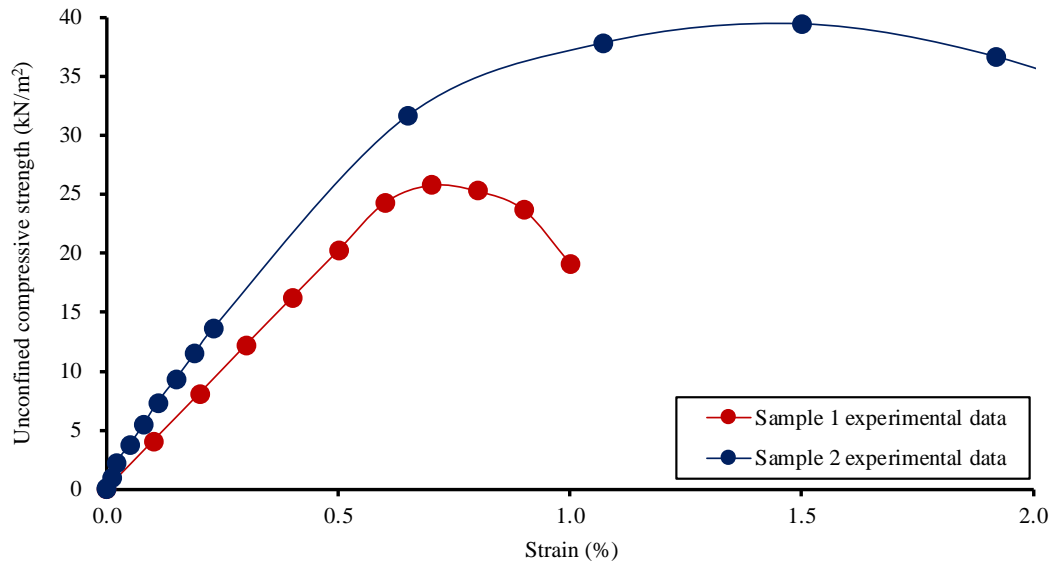
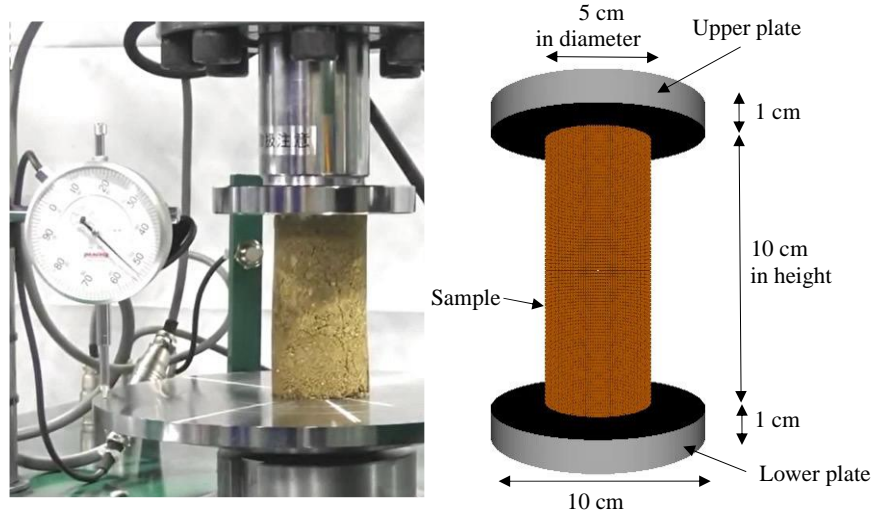


Figure 2. Experimental stress-strain curve characteristics of Samples 1 and 2

## 2.2. Methodology

The method of study in this research is to reproduce the unconfined compression test (UCT) phenomenon through a simulation that utilizes computer-aided engineering (CAE) technology to create the model and the moving particle semi-implicit (MPS) method as the numerical calculation method. Then, an attempt is made to reproduce the output results that will be equivalent to the benchmark UCT results described in Section 2 as closely as possible. This study will focus on identifying the probable influencing parameters and their sensitivity in the simulation through a trial-and-error process. Figure 3 shows the analysis model for Sample 1 and the experimental model at the approximate yield point of the unconfined compression test. As indicated by the details in Table 1, this study will utilize two different samples with different dimensions. Therefore, it is mandatory that two different analytical models be created with dimensions exactly equal to those of the experimental sample.



**Figure 3. Illustration of analysis model and experimental model setup for Sample 1**

Computer-aided engineering (CAE) represents technology that allows users to conduct large-scale experiments by adopting prototypes created by CAD (computer-aided design) to analyze and simulate experiments under various site conditions. The analysis model for this study was created using AutoCAD.

The moving particle semi-implicit (MPS) method is a numerical analysis method used to simulate incompressible fluid; it analyzes the behavior of fluid particles using a semi-implicit algorithm [28, 29]. This method does not use the grid method for the calculation points. Rather, it uses the particle method, in which the domain is discretized into a physical quantity that holds data related to the physical characteristics, pressure, and velocity. In this method, the particles move at each calculation point in a Lagrangian manner, leading to solutions to the governing equations for incompressible fluids. The mass conservation law and Navier's stroke law are the governing equations; they are shown in Equations 1 and 2, respectively.

$$\frac{D\rho}{Dt} = 0 \quad (1)$$

$$\frac{Du}{Dt} = -\frac{1}{\rho}\nabla P + \vartheta\nabla^2 u + g + \frac{1}{\rho}\sigma k\delta n \quad (2)$$

where  $\rho$  is the density of the fluid,  $t$  is time,  $u$  is the velocity vector,  $P$  is pressure,  $\vartheta$  is the kinematic viscosity coefficient,  $g$  is the gravity vector,  $\sigma$  is the surface tension coefficient,  $k$  is the interface curvature (positive if the center of the curvature is on the side of liquid),  $\delta$  is the delta function for the surface tension acting on the surface, and  $n$  is the unit vector in the direction perpendicular to the surface.

Figures 4-a and 4-b show a comparison of schematic diagrams for the Bingham fluid model and the bi-viscosity Bingham model, respectively. Bingham fluids are types of fluid that will begin to flow only when the shear stress value exceeds a certain value; otherwise, they remain immobile. In the context of an MPS simulation, Bingham fluid is regarded as a viscoplastic fluid when it exhibits fluid-like behavior and as a highly viscous fluid when it is in a rigid state. The constitutive equations, Equations 3 and 4, represent the fluid state and the rigid state, respectively, of the bi-viscosity model of Bingham fluid.

$$T_{ij} = -P\delta_{ij} + 2\left(\eta_p + \frac{\tau_y}{\sqrt{\Pi}}\right)\dot{\epsilon}_{ij}^{vp} \quad \Pi > \Pi_c \quad (3)$$

$$T_{ij} = -P\delta_{ij} + 2\left(\eta_p + \frac{\tau_y}{\sqrt{\Pi_c}}\right)\dot{\epsilon}_{ij}^v \quad \Pi < \Pi_c \quad (4)$$

where  $P$  is pressure,  $\delta_{ij}$  is Kronecker's delta,  $\eta_p$  is the plastic viscosity,  $\tau_y$  is the yield value,  $\dot{\epsilon}_{ij}^{vp}$  is the strain rate while in the fluid state,  $\dot{\epsilon}_{ij}^v$  is the strain rate while in the rigid state,  $\Pi$  represents at what rate the deformation tensor occurs, and  $\Pi_c$  is the yield reference value used to determine whether the soil is in the fluid state or the rigid state. It should be noted that  $\Pi$  and  $\Pi_c$  are expressed by Equations 5 and 6, respectively, using the flow limit strain rate. They express the stress-strain relationship for the Bingham fluid bi-viscosity model.

$$\Pi = 2\dot{\epsilon}_{ij}\dot{\epsilon}_{ij} \quad (5)$$

$$\Pi_c = (2\pi_c)^2 = \left(\frac{2C_y\tau_y}{\eta}\right)^2 \quad (6)$$

where,  $\dot{\epsilon}_{ij}$  is the rate of the deformation tensor,  $i$  and  $j$  are the indices denoting the spatial dimensions,  $\pi_c$  is the critical shear strain,  $\eta$  is the plastic viscosity,  $\tau_y$  is the yield value, and  $C_y$  is the yield parameter.

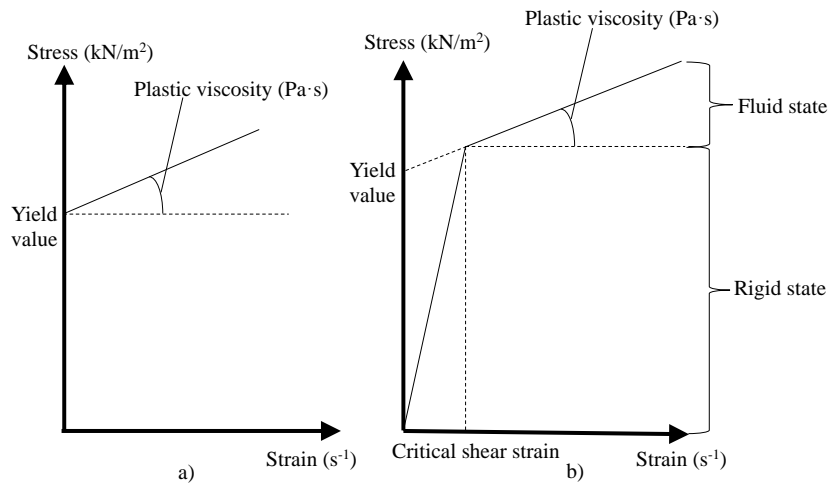
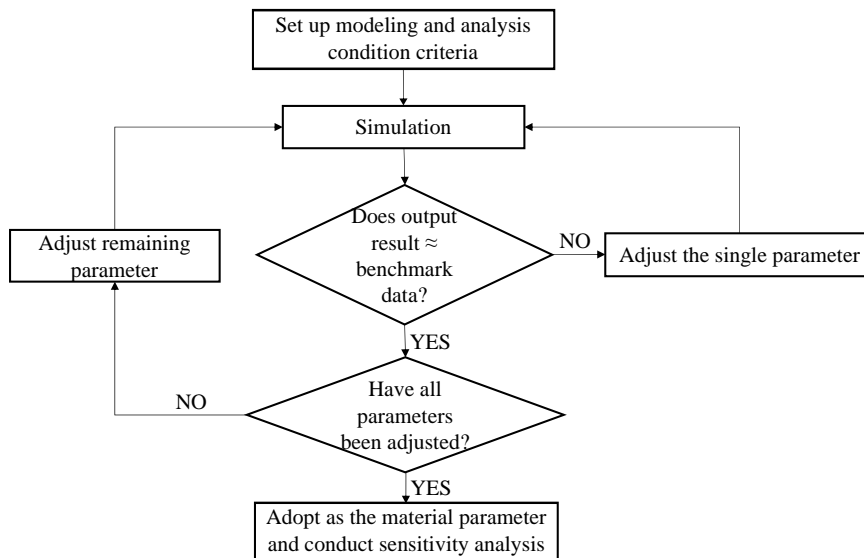
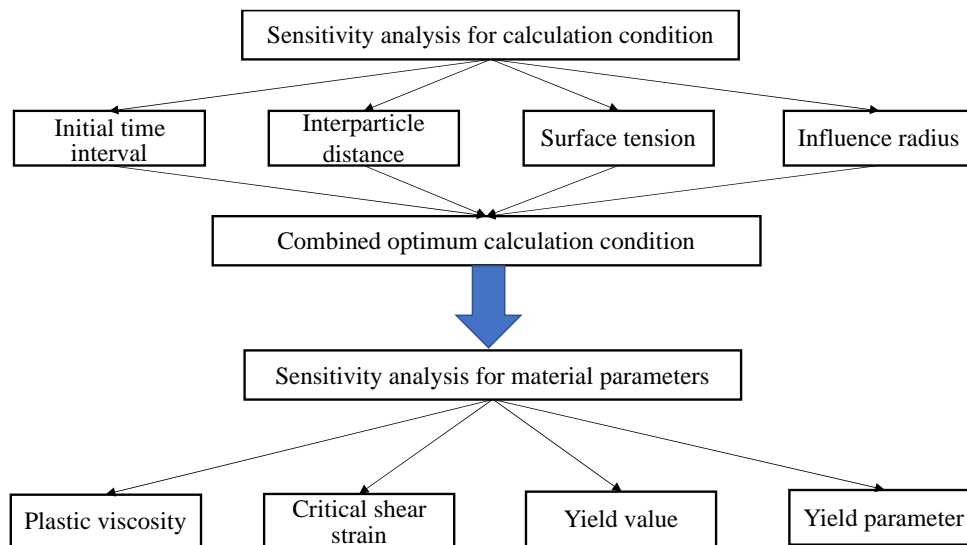


Figure 4. Schematic diagrams comparing Bingham fluid model and bi-viscosity Bingham model

Using an MPS-CAE simulation, an attempt was made to reproduce the exact benchmark unconfined compression test data through a number of trial-and-error simulations. Figure 5 provides a flowchart of the MPS-CAE simulation.



(a) Flowchart of MPS-CAE simulation by trial-and-error



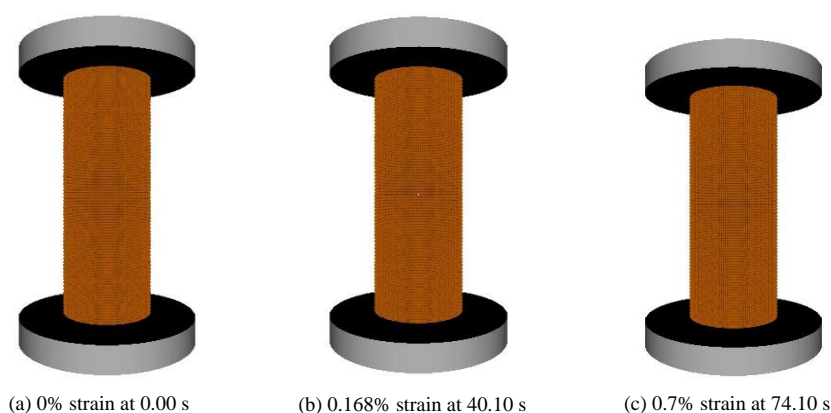
(b) Flowchart of sensitivity analysis by MPS-CAE simulation

Figure 5. Flowchart diagrams of MPS-CAE simulations

### 3. Analysis Conditions

This section will describe the pre-simulation process up to the point of the initialization of the simulation. Firstly, the animation for the UCT procedure is created using the objects determined by CAE. A setup comprising a top plate and a bottom plate represents the UCT apparatus, and uniform compression is applied to the soil sample placed between these plates by lowering the upper plate. The plates were assigned as a polygon during the simulation with wall friction such that the specimen would not experience the slip condition. The bottom plate remained stationary throughout the simulation; only the top plate underwent constant downward motion, such that the soil sample experienced strain at 1% per minute. The specimen placed between these plates should make contact with both plates without exerting any pressure on them, so that there will not be any additional strain on the specimen.

Figure 6 shows the three different simulation stages of the analysis given in Figure 3, depicting the strain values of 0%, 0.168%, and 0.7% at 0s, 10.1s, and 42.1s, respectively. This particular analysis model for Sample 1 shows a yield point of approximately 42.1s. Unlike the experimental sample, the simulation soil sample shows only a compressed version instead of a fracture. However, the yield point can be confirmed by plotting the stress-strain curve from the output data. The additional detailed analysis conditions are described in the following two subsections. The first subsection discusses the calculation method selected for this study with an explanation, while the second subsection discusses the analysis of parameter values in detail.



**Figure 6. Illustration depicting progress of analytical model at different strain values**

#### 3.1. Method of Calculation

In the MPS simulation, Navier's Stroke law and mass conservation law are the governing equations, where pressure, viscosity, and surface tension are the major parameters. Therefore, it is important to adopt the proper calculation method for each parameter during the setup of the simulation. Calculation of the pressure and viscosity can be done with either the implicit method or the explicit method [30–33]. However, in this simulation, both parameters were calculated with the implicit method because the calculation was carried out in several time increments, and the overall analysis results of the simulation were determined by the calculation results at each time increment in the MPS method. In the explicit calculation method, the calculation of a future value is carried out based on its current value and the values of its derivatives at that point in time. In other words, the future value of a function is calculated directly with this method based on the known values of the function and its derivatives, without the need to solve any additional equations or perform any numerical integration [34]. Therefore, it is a simple and easy method to implement. However, the calculation might not converge in the case of increasing the time increment because the particles might scatter beyond their expected positions. With the implicit calculation method, however, the calculation of the future value is carried out based on the solution of a function by solving a set of equations that involve both the current and future values of the function. It follows that the memory capacity required for this method is larger, but it does not require making the time steps as small as those required with the explicit method to attain accuracy. Thus, the overall total computation time is reduced for a more precise calculation. Moreover, in the pressure calculation, the explicit method is used for compressible fluids in which deformation is caused by an external compressive force and the effect of hydrostatic pressure is negligible. Meanwhile, the implicit method is used for incompressible fluids in which the effect of hydrostatic pressure is not negligible. Since the MPS method assumes the fluid to be an incompressible fluid, the implicit method is adopted for the pressure calculation in this simulation. In the calculation of viscosity, the explicit method is used for low-viscosity fluids that change positions significantly with each time increment. Meanwhile, the implicit method is used for the calculation of high-viscosity fluids. Since the specimens were assumed to be highly viscous fluids, the implicit method was adopted for the viscosity calculation in this simulation. In addition, the numerical stability of the simulation is compromised unless Equations 7 and 8 are satisfied for the explicit calculation of pressure and viscosity, respectively, which are not met in this study.

$$r \ll c \times \Delta t \quad (7)$$

$$\Delta t < 0.2 \times \frac{r^2}{\eta} \quad (8)$$

where  $\Delta t$  is the time step,  $r$  is the interparticle distance,  $c$  is the speed of sound, and  $\eta$  is the plastic viscosity.

As for surface tension, it can be calculated by either CSF or the potential method. However, the soil specimens used in this simulation are not ideal fluids but are assumed to be samples of the bi-viscosity model of Bingham fluid, which exists in both rigid and fluid states. Also, the attractive intermolecular force, like the van der Waals force, responsible for the surface tension, is lower than the surface hydration repulsive force for particle distances greater than 1.4 nm. For soil containing a low water content, the repulsive electrostatic force is high [35]. Considering the low water content and higher particle distance in the samples used in this simulation, it was assumed that the influence of surface tension would be for the unconfined compression tests of the soil samples, as they would remain in the rigid state of the bi-viscosity model [26]. Thus, the calculation of surface tension is omitted in this study by assigning the calculation method as none.

### 3.2. Analyzing Parameter Values

The wet density measured during the experiment for each specimen was used as the input value for the density during the simulation. The distance between particles and the initial time interval for the simulation have a significant impact on the accuracy and time required for the analysis. Therefore, the initial study was focused on determining the optimum interparticle distance value and initial time interval value before an analysis was conducted to determine the value of the Bingham fluid parameter. Table 2 summarizes the physical properties of Sample 1, the mode of calculation for the MPS simulation, and the optimum simulation parameters used in the analysis conditions of this sample to study the influence of the interparticle distance and initial time increments. The values for the yield value, plastic viscosity, yield parameter, and critical strain rate were selected based on the results generated by the previous trial-and-error simulations. For the parameters that are not included in Table 2, default values were used. The optimum values for the initial time interval and interparticle distance were determined after studying their influence both separately and in combination.

**Table 2. Analysis conditions of Sample 1**

MPS (Mode of calculation)	Pressure	Type Mode	Implicit Stabilized
	Viscosity	Type	Implicit
		Beta	1
	Surface tension	Type	None
Optimum simulation parameters	Particle size	0.5 mm	
	Initial time interval	0.05 s	
	Finish time	90 s	
Physical properties	Density	1668 kg/m <sup>3</sup>	
	Surface tension coefficient	0.002 N/m	
	Yield value	12.900 kN/m <sup>2</sup>	
	Plastic viscosity	8600 Pa·s	
	Yield parameter	0.0001	
	*Critical shear strain	0.000129 s <sup>-1</sup>	

\* Not inputted directly, but used for calculating other values.

## 4. Results and Discussion

### 4.1. Determination of Optimum Interparticle Distance and Initial Time Interval

In the particle method, the particles are the calculation points used for the fluid description, and the distance between these calculation points is called the interparticle distance. When the interparticle distance values are decreased, the number of calculation points increases proportionately, and when the initial time interval is decreased, the number of times the calculations must be conducted increases. This will result in an exponential increase in the overall calculation load and duration. The simulation itself is limited by the number of calculation points that it can incorporate into the analysis before coming to a halt due to the massive calculation load. Thus, the precision of the simulation results depends on the input values for the interparticle distance and initial time interval, and hence, this study was conducted to determine the most appropriate analytical conditions.

Figure 7 shows the simulation results for the different values of interparticle distance compared with the experimental stress-strain relationship of Sample 1. The initial time interval for every calculation was set to be 0.05 s. The simulation was conducted for 0.9 mm and gradually continued to check for lower values, finally stopping at 0.5 mm due to the time constraint. The result for the 0.9-mm interparticle distance shows the lowest unconfined compressive strength and highest strain value. A clear pattern can be seen in the output results as the unconfined compressive strength value continues to increase and the strain value continues to decrease for the lower interparticle distance. For the 0.5-mm interparticle distance, the unconfined compressive strength is seen to be maximum with the unconfined compressive strength value of 27.16 kN/m<sup>2</sup> and strain value of 0.9%. However, it should be noted that the unconfined compressive strength for the 0.7-mm interparticle distance is only 23.48 kN/m<sup>2</sup>, but the strain value is 0.82%, slightly lower than that of 0.5 mm. This slight change in pattern after 0.7 mm, whereby the unconfined compressive strength continues to increase and afterward the strain value starts to slightly increase, could be attributed to an increase in the precision of the analysis due to increments in the calculation points in the system accompanying the decrease in interparticle distance.

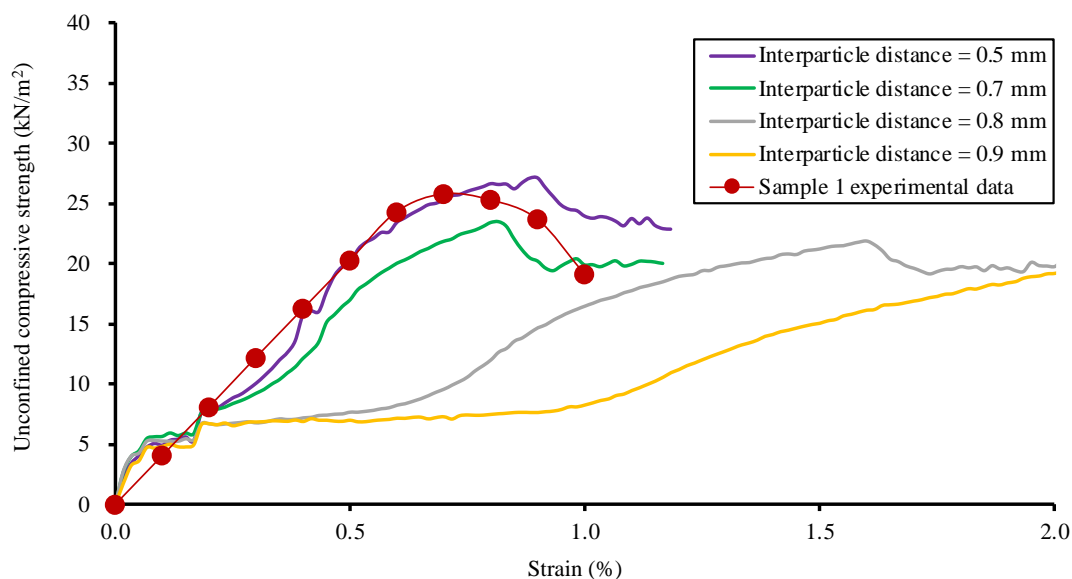


**Figure 7. Comparison of simulation output results for different interparticle distances**

This simulation was modeled after Sample 1, which has an unconfined compressive strength of 25.8 kN/m<sup>2</sup> at a strain value of 0.7%. From this comparative analysis, the result for the 0.5-mm interparticle distance was the most closely reproduced result judging by the curve characteristics and unconfined compressive strength. The result for the 0.7-mm interparticle distance also shows similar characteristics with lower unconfined compressive strength and strain values. The strain value is slightly more accurate, but the unconfined compressive strength is still lower than the benchmark comparison value. It is observed that the fluctuation in the strain value becomes lower when the input parameter values start resembling the correct value. However, the output unconfined compressive strength still shows a comparatively remarkable fluctuation despite the input parameters starting to resemble the correct values. Thus, it is possible to obtain different values for the unconfined compressive strength with the same strain value. Therefore, the output unconfined compressive strength value is more reliable for use as a benchmark, and higher emphasis is given to determining the precision of the simulation. In relation to a future study, it is important to note that the strain value decreases for a lower interparticle distance and, after a certain value, it increases slightly.

The simulation for the 0.5-mm interparticle distance was conducted before that for the 0.6-mm interparticle distance and, upon observing the results, it was found that the output unconfined compressive strength and strain values are refined and the curve characteristics partially overlap the experimental results, especially at the yield points. From the overall result pattern, the 0.6-mm interparticle distance most likely produces the more accurate output unconfined compressive strength and strain values, but the curve overlapping the benchmark curve will probably be less than that for the 0.5-mm interparticle distance. Moreover, it is important to remember that other parameters inputted in this simulation have not yet been discussed, including the initial time interval. It is also important to note that the overall results might change depending on the input values of the other parameters. Thus, the absence of the 0.6-mm interparticle distance might not make much of a difference at this phase. Hence, considering the time constraint and the achievement of acceptable results at this phase, the simulation for the 0.6-mm interparticle distance was skipped.

Figure 8 shows the simulation results of Sample 1 for the different values of the initial time interval. The study was conducted for the initial time interval values of 0.005 s, 0.006 s, 0.007 s, and 0.008 s. The interparticle distance for this

simulation was set to be 0.5 mm and all other parameters were the same as those given in Table 1. The initial time interval value was directly inputted in the parameter setting for the simulation which would be treated as the value of the time increment in the calculation. For the smaller value of the initial time interval, the particles that act as calculation points are constrained within the boundary walls and are bounced off the walls whenever the calculation results try to diverge. In addition, the distance traveled by the particles at each time increment will be limited, resulting in an increase in the accuracy of the analysis by decreasing any errors at the next time increment. However, the calculation time may increase drastically depending on the input value of the initial time interval. Thus, it is necessary to adopt the optimum value for the initial time interval.

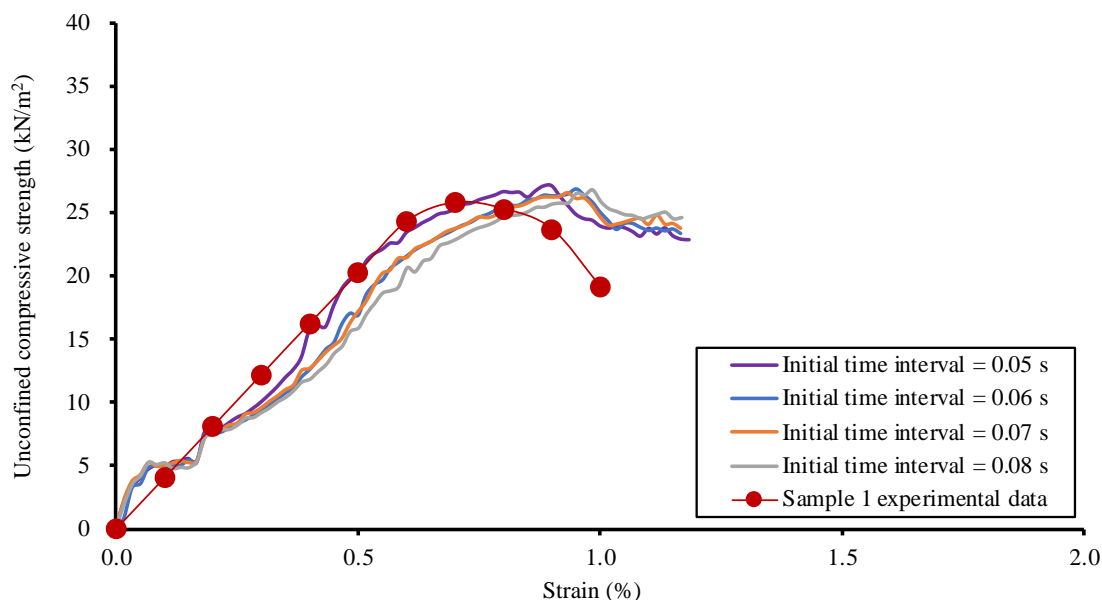


**Figure 8. Comparison of simulation output results for different initial time intervals**

It was observed that the output values for the unconfined compressive strength and strain were almost equivalent for all simulations with just a slight increase in unconfined compressive strength, and that a lower value was seen for the initial time interval with a slight decrease in the value for strain. Initial time intervals below 0.05 s were not studied here due to the time constraint. Moreover, judging from the results, the curve characteristics started resembling the target curve characteristics, indicating that the initial time intervals that had been selected for this study were already within the permissible range for reproducing results without much deviation. Therefore, considering the time required for the calculation and other factors, it is recommended that the value of the initial time interval be selected based on the allowable time frame in future studies.

Both the interparticle distance and initial time interval both have a significant impact on the accuracy of and time required for the analysis, influencing the calculation load. Therefore, the influence of these two parameters must be studied simultaneously and checked to see if they deviate from the expected results. Additionally, since these values are not the actual parameters for the MPS simulation model, but the parameters on which the calculation is carried out for any model, it is necessary to establish a proper guideline for future reference. Therefore, an attempt was made here to establish the optimum values for the initial time interval and interparticle distance for any type of MPS simulation.

Figure 9 shows the simulation results for Sample 1 for the different combinations of interparticle distance and initial time interval, as given in Table 3. The simulation showed that the most accurate result was obtained for the combination of the 0.5-mm interparticle distance and the 0.05-s initial time interval. The unconfined compressive strength value of 27.16 kN/m<sup>2</sup> and strain value of 0.9% were obtained for Case I. The results for Case II could also be considered as reliable outputs as the unconfined compression strength of 23.03 kN/m<sup>2</sup> and strain value of 0.87% were obtained, which are almost equivalent to the target values of Sample 1. On the other hand, Figure 7 shows that the 0.7-mm interparticle distance simulated at the initial time increment of 0.05 s produced the unconfined compressive strength of 23.48 kN/m<sup>2</sup> at the strain value of 0.82%. These results indicate that emphasis should be placed on decreasing the interparticle distance rather than the initial time interval if there is a time constraint in the study for higher precision of the results. In addition, it can be concluded that MPS simulations conducted for interparticle distances lower than 0.7 mm and initial time intervals lower than 0.07 s produce the optimum results, and that the selection of values should be done according to the study conditions.

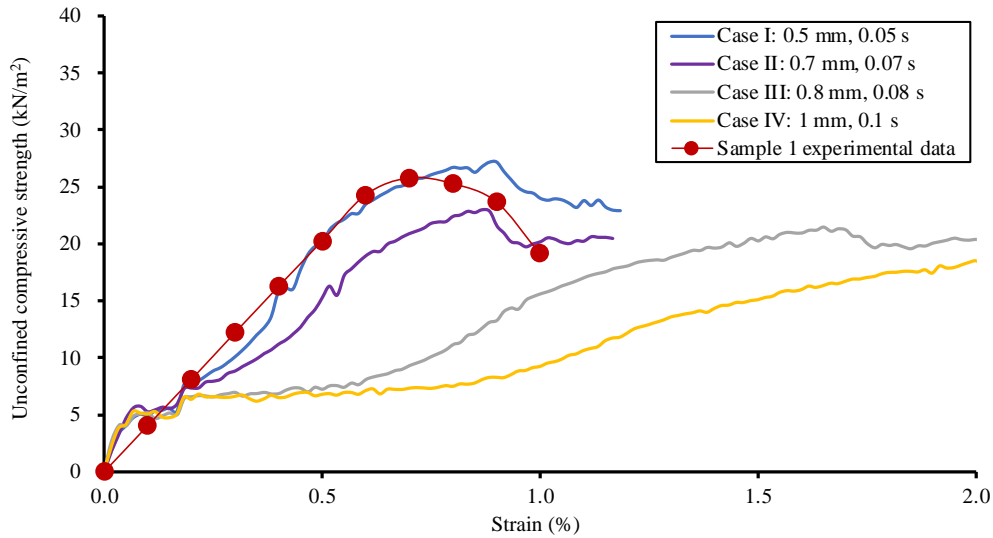


Figure 9. Simulation results for different combinations of interparticle distance and initial time interval

Table 3. Different combinations of interparticle distance and initial time interval for Sample 1

Case	Interparticle distance (mm)	Initial time interval (s)
I	0.5	0.05
II	0.7	0.07
III	0.8	0.08
IV	1.0	0.10

Figure 10 depicts an image of the interparticle distance ( $r$ ) and radius of influence ( $R$ ). The distance from the center of one particle can influence the other particles. The distance determines the number of particles inside the fluid that are affected by this situation. In the MPS method, the major components of the governing equations, like pressure, particle velocity, viscosity, and surface tension, affect the particle method calculations. The components of these governing equations that control the MPS simulation are discretized using a weighting function in accordance with Equation 9.

$$w(r) = \begin{cases} \frac{R}{r} - 1 & (0 \leq r \leq R) \\ 0 & (R \leq r) \end{cases} \tag{9}$$

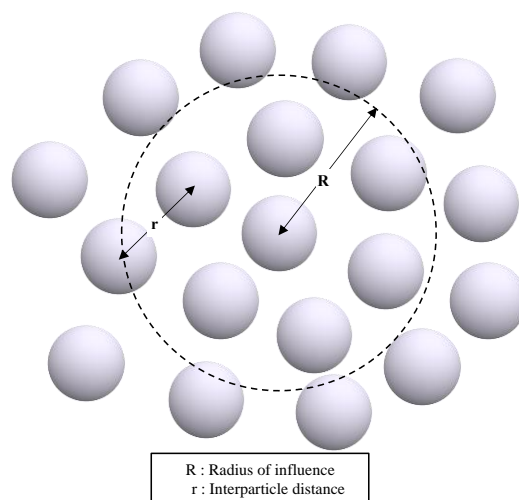


Figure 10. Interparticle distance and radius of influence of particles

The pressure value of the particles at the free surface of the fluid is fixed at zero as a directory boundary condition of the pressure Poisson equation in the MPS method, but the pressure values of the particles inside the fluid have different values [36]. The degree of influence on the particles inside the fluid is determined by the value of the influence radius. The influence radius ( $R$ ) is 2.1 to 4.1 times the interparticle distance ( $r$ ). Normally, the standard value of the influence

radius is 3.1. It is recommended that this value not be changed under normal conditions, as it will reproduce less accurate results. This was verified when the influence radius value was changed for pressure and/or viscosity, as the results were skewed from an acceptable pattern. However, the change in surface tension showed the correct pattern of results with almost equivalent or only slightly different output values. At the setting of the MPS simulation, the assumption was made that the surface tension force acting on the surface of the soil sample was negligible, and thus, was not included in the calculation. However, the same condition cannot be applied to other fluids with sufficient mobility. Since the objective of this study is to establish the basic simulation parameter values for the MPS simulation, all probable scenarios must be established. Thus, the authors have attempted to study the changes in the patterns of the output results for different values of influence radius in surface tension.

Figure 11 presents the yielding stress and strain results for Sample 1 for the different values of influence radius for the surface tension. The simulation was conducted for the interparticle distance of 0.5 mm and initial time interval of 0.05 s for all values of influence. Increasing the value of the influence radius had almost no impact on the results, and almost the same output values for strength and strain were obtained for any time. However, a decrease in the value of the influence radius produced slightly different results. It was more accurate in terms of both the strength and strain values with the output unconfined compressive strength of 26.16 kN/m<sup>2</sup> at the strain value of 0.82%. This suggests that lowering the influence of surface tension increases the precision of the results, which proves that the initial assumption of surface tension having a negligible influence on the soil specimen in the unconfined compression test was true. It might raise the question as to whether or not the results were improved because of the initial assumption of the surface tension being negligible. However, the fact that increasing the value of the influence radius did not impart any influence disapproved the initial assumption.

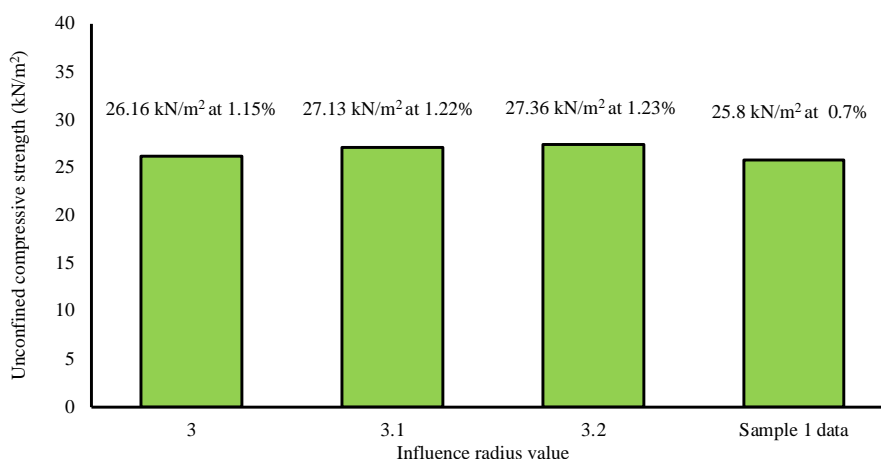


Figure 11. Simulation results of Sample 1 for different values of influence radius in surface tension

#### 4.2. Sensitivity Analysis of Parameters Related to Bi-Viscosity Model

The major influencing parameters of the bi-viscosity model are plastic viscosity, yield value, critical shear strain, and yield parameter, as defined in Equation 6. The yield value for the simulation was taken to be half of the uniaxial compressive strength of the sample [27]. In addition, it was hypothesized that the yield value in the bi-viscosity model corresponds to the shear strength and equals approximately half the unconfined compressive strength according to Mohr's Coulomb failure criteria [8]. However, a simulation was conducted to verify whether or not this would be true for the simulation parameters in this study. A study for the yield parameter has already been done [26]; thus, the present study will not conduct a separate study for the sensitivity analysis of the yield parameter. As for the remaining parameters, a sensitivity analysis for both Samples 1 and 2 was performed. The simulation was conducted with the MPS setting of an interparticle distance of 0.5 mm, initial time interval of 0.05 s, and radius of influence of 3.1 times.

Figures 12 and 13 show the results of the sensitivity analysis of Samples 1 and 2, respectively, for the plastic viscosity, compared to their respective target data characteristics at different strain values. The yield value of 12.9 kN/m<sup>2</sup> and critical strain rate of 0.000129 s<sup>-1</sup> were set for Sample 1. Meanwhile, the yield value of 19.743 kN/m<sup>2</sup> and critical strain rate of 0.00012 s<sup>-1</sup> were set for Sample 2. In both cases, the values for the yield parameter were adjusted in order to change the values of the plastic viscosity. Table 4 presents the cases of the analysis conditions used for this sensitivity analysis. However, the results for both cases confirm that the influence of this particular directly proportional relationship of plastic viscosity and yield parameter might be negligible in the generation of the output results. It was found that the output results were almost equivalent for all plastic viscosity values of both samples when the yield value and critical shear strain were kept constant. Therefore, it is impossible to determine the plastic viscosity value under these analysis conditions; it needs to be studied in detail for other patterns of analysis conditions. The plastic viscosity

is expected to have a directly proportional relationship with the yield parameter, as suggested by Equation 6. However, it might be possible that the plastic viscosity value is linked to the yield parameter value by a negligible amount only. Therefore, it becomes essential to establish the influence of the dependency of the plastic viscosity value on other parameters in order to determine the exact value.

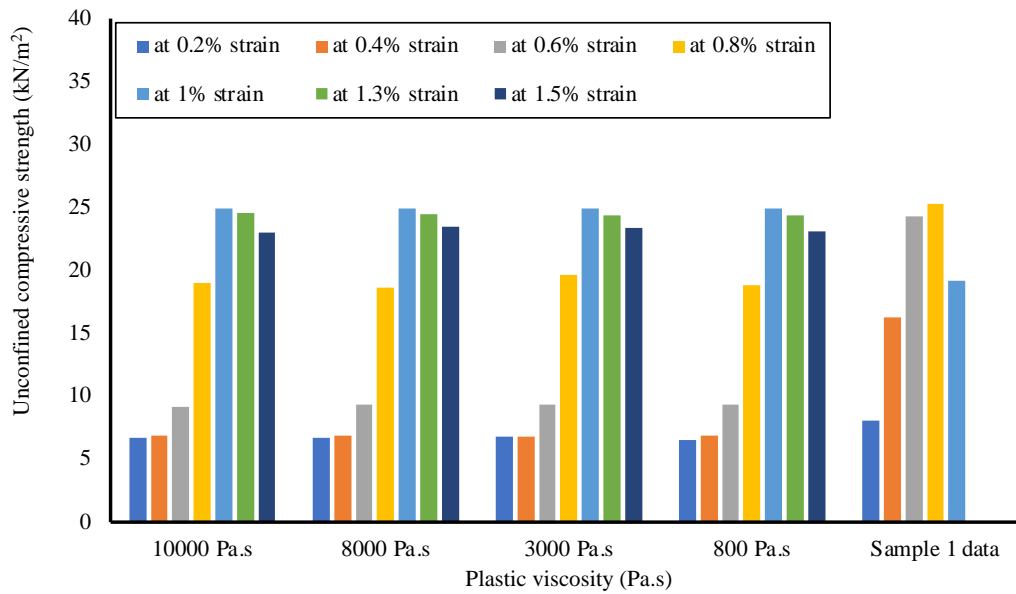


Figure 12. Sensitivity analysis results of plastic viscosity for Sample 1 at different strain values

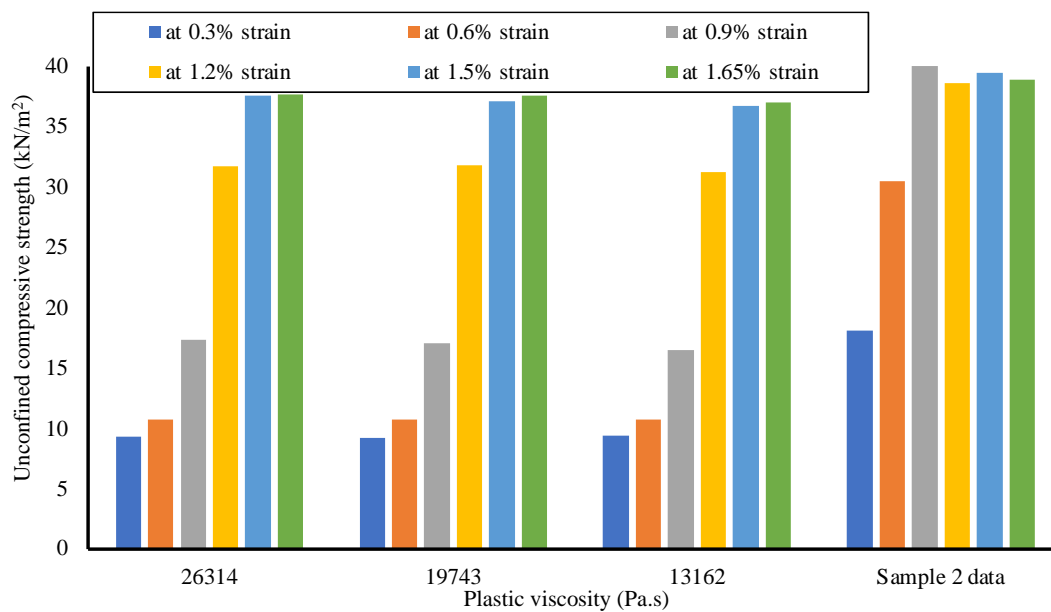


Figure 13. Sensitivity analysis results of plastic viscosity for Sample 2 at different strain values

Table 4. Conditions for plastic viscosity sensitivity analysis

Sample	Other parameters	Plastic viscosity (Pa.s)	Yield parameter
1	Yield value = 12.9 kN/m <sup>2</sup> Critical strain rate = 0.000129 s <sup>-1</sup>	10000	0.0001
		8000	0.00008
		3000	0.00003
		800	0.000008
2	Yield value = 19.743 kN/m <sup>2</sup> Critical strain rate = 0.00012 s <sup>-1</sup>	26324	0.00016
		19743	0.00012
		13162	0.00008

In a previous study, Shakya & Inazumi [26] concluded that plastic viscosity has a directly proportional relationship with the unconfined compressive strength if the yield value and yield parameter are kept constant. It can be inferred that the plastic viscosity value, when changed by adjusting the critical shear strain, significantly influences the output results.

Therefore, it can be deduced that the plastic viscosity is influenced by the critical shear strain. This case will be discussed further in a sensitivity analysis of the critical shear strain, in which the critical shear strain value will be changed by adjusting the plastic viscosity. Next, to deduce the relationship between plastic viscosity and the yield value, it is important to notice the relation between plastic viscosity and the unconfined compressive strength. Since an increase in plastic viscosity results in an increase in unconfined compressive strength [26], and the fact that the yield value is generally taken as half the unconfined compressive strength [27], it can be concluded that the yield value is influenced in a direct proportional relationship by the plastic viscosity, which is in agreement with the concept suggested by Equation 6. However, when the particle sizes are changed, the same output unconfined compressive strength value is obtained for the much lower value of plastic viscosity [14]. Hence, it can be further deduced that this particular direct proportional relationship might only be moderately influential on the output results. Therefore, it is highly probable that linking the values of the plastic viscosity and critical shear strain together might be the most highly influential analysis pattern in the output results.

Figures 14 and 15 show the sensitivity analysis results for Samples 1 and 2, respectively, for different critical strain rate values. In this sensitivity analysis, the yield parameter and yield value were kept constant, and the values for plastic viscosity were adjusted in order to change the critical shear strain value for the Sample 1 model. Meanwhile, the yield value and plastic viscosity were kept constant, and the values for the yield parameter were adjusted in order to change the critical shear strain for the Sample 2 model. It has already been proven, from the results of Figures 12 and 13, that the result pattern will be the same, regardless of the simulation model, if the analysis conditions are constant and the varying parameter types are the same. For these sensitivity analyses, the yield value was selected as half of the unconfined compressive strength.

For Sample 1, a sensitivity analysis was conducted with a yield value of  $12.9 \text{ kN/m}^2$  and yield parameter of  $0.0001$ , and the value of the plastic value was adjusted in order to change the critical shear strain value rate based on Equation 6. It was deduced that this relationship should greatly influence the output results based on the study by Shakya & Inazumi [26], which was proven to be true, as shown in Figure 14. It was observed that the most accurate result was obtained for the critical strain rate value of  $0.000129 \text{ s}^{-1}$ . However, the critical strain values of  $0.000108 \text{ s}^{-1}$  and  $0.000086 \text{ s}^{-1}$  also provided satisfactory results. The value of the unconfined compressive strength increased and the strain value decreased for the lower value of critical shear strain. On the other hand, the critical shear strain value around  $0.000258 \text{ s}^{-1}$  was not even similar to the correct curve characteristics of Sample 1. Thus, it may be deduced that the correct value for the critical shear strain might be around  $0.000129 \text{ s}^{-1}$ .

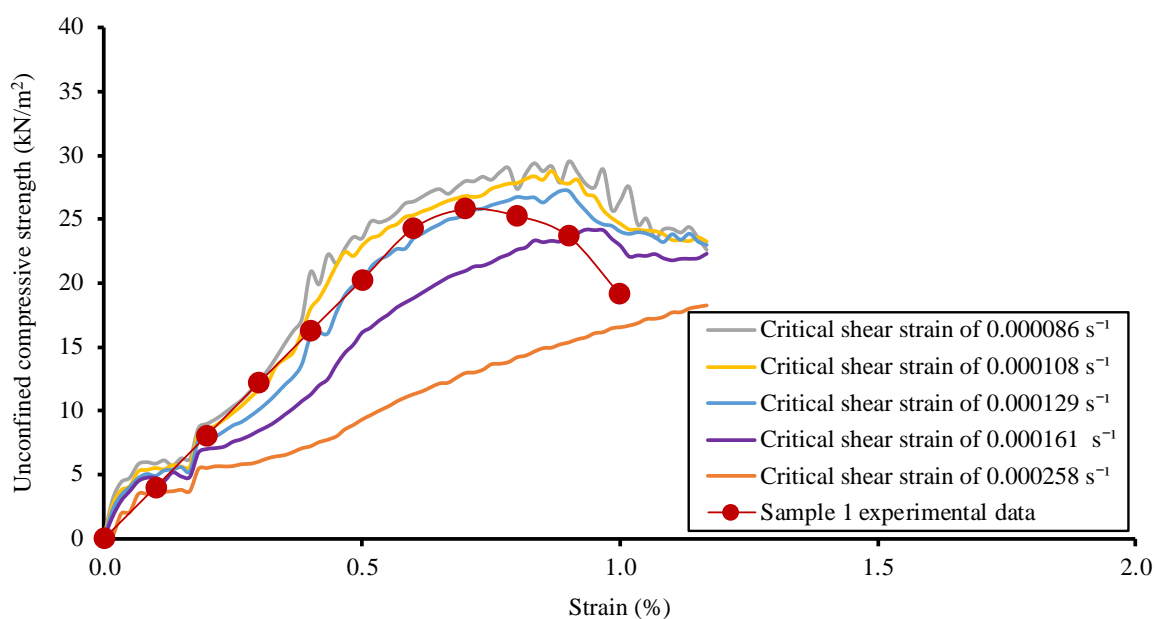
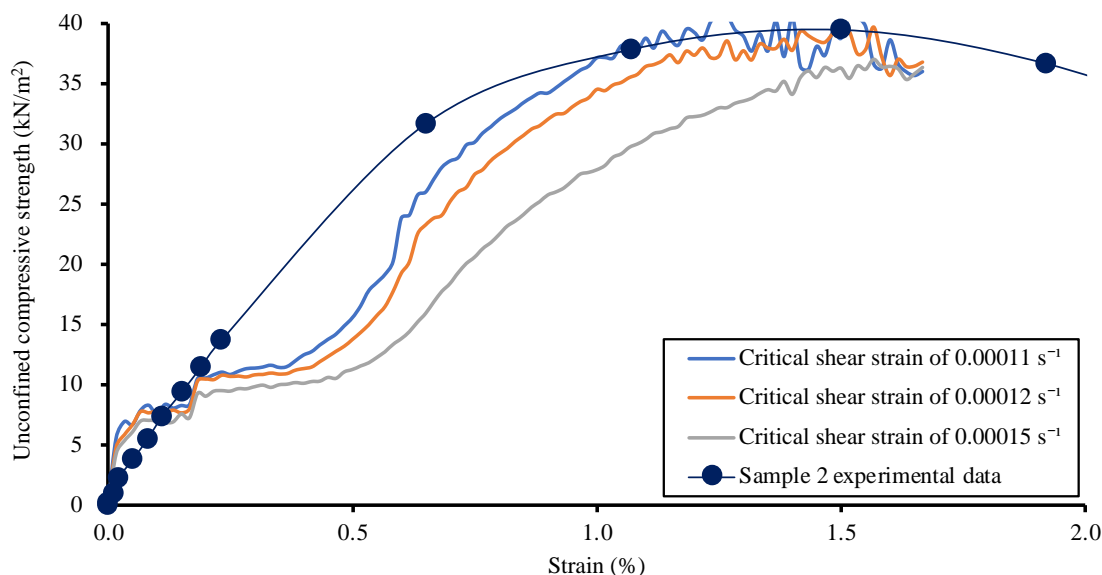


Figure 14. Patterns of sensitivity analysis results for critical shear strain in Sample 1



**Figure 15. Patterns of sensitivity analysis results for critical shear strain in Sample 2**

Meanwhile, for Sample 2, a sensitivity analysis was conducted with a yield value of  $19.743 \text{ kN/m}^2$  and plastic viscosity value of  $13162 \text{ Pa}\cdot\text{s}$ , and the value of the yield parameter was adjusted to change the values of the critical shear strain. The reason for selecting the yield parameter as the parameter to be adjusted, in order to change the critical shear strain, was to compare the degrees of influence for different sets of varying and constant parameters in the sensitivity analysis. Shakya & Inazumi [26] provided the general guideline for selecting the values for the yield parameter. The simulation itself was successful for yield parameter values below  $1/1000$  only, namely, values below  $1/10,000$  imparted very little influence, but a similar result pattern [26]. A similar pattern in the critical shear strain sensitivity analysis results was observed for Sample 2 where the accuracy of the stress-strain curve increased for lower values of critical shear strain. As for the yield parameter values, they were selected as  $0.00007$ ,  $0.00008$ , and  $0.0001$  for the critical shear strain values of  $0.00011 \text{ s}^{-1}$ ,  $0.00012 \text{ s}^{-1}$ , and  $0.00015 \text{ s}^{-1}$ , respectively. The conclusion by Shakya & Inazumi [26], regarding a yield parameter value around  $1/10000$ , that provides the optimum result, was verified by this result, as it can be observed that the precision of the result increased for the lower values of the yield parameter value, but still approximately equaled  $1/10000$ . However, it is also important to note the degree of influence when studying the sensitivity analysis. It can be observed that the stress-strain curve characteristics do not exactly resemble the benchmark curve characteristics, unlike what was seen for the other assessment results. This indicates that the direct relationship of the critical shear strain and the yield parameter might only be moderately influential on the output results. As for the adjusted sensitivity analysis with the remaining yield value, no study was conducted because the yield value will be known for a known soil sample and, if necessary, the influence on the output results can be deduced from the pattern of previous results. The critical shear strain and yield value should have a direct proportional relationship, but their influence on the output results might be negligible. It has already been established that the critical shear strain, linked with the plastic viscosity as the varying parameter, has the highest influence. And, a similar pattern of the yield value linked with the yield parameter must be the most influential on the output results. This hypothesis will be checked and discussed in a sensitivity analysis of yield values.

It is important to notice that the critical shear strain value of  $0.000108 \text{ s}^{-1}$  for Sample 1 and the critical shear strain value of  $0.00011 \text{ s}^{-1}$  for Sample 2 provided satisfactory results, but not the most optimum results. This is approximately  $1/100$  times the magnitude of the experimental strain values for Sample 1 ( $0.7\%$ ) and Sample 2 ( $1.67\%$ ). This was the pattern observed for the samples utilized in this study only; thus, it might not hold true for all incompressible fluids and cannot be established as a standard relationship. However, it can be useful as a time-reducing guideline to determine the actual material parameter.

Figure 16 shows the output results for the sensitivity analysis of Sample 1 for the yield value. Although the general theory behind the selection of the yield value, as half of the unconfined compressive strength, has already been established [27], the simulation for Sample 1 was conducted to verify the results. The input values for the plastic viscosity and critical shear strain were kept constant throughout the simulation, and the value for the yield parameter was adjusted for each simulation based on Equation 6. It was observed that the unconfined compressive strength and strain values increased with an increase in the yield value, but the optimum value was observed for the value equal to half of the unconfined compressive strength. Hence, these findings prove that the results determined for the other sensitivity analysis are also true. Here, the previous hypothesis made about the yield value, when adjusted with the yield parameter, imparts the greatest influence on the output results during the sensitivity analysis of the critical shear strain

also proven to be true. Therefore, it is recommended that the yield value be linked with the yield parameter, and the plastic viscosity with the critical shear strain, to determine the exact value of each parameter during the simulation. Table 5 presents a summary of the conditions used in the sensitivity analysis. Meanwhile, Table 6 shows a summary of the inter-relationship between each major parameter of the Bingham fluid bi-viscosity model based on the theoretical relationship and observed influence on the simulation results.

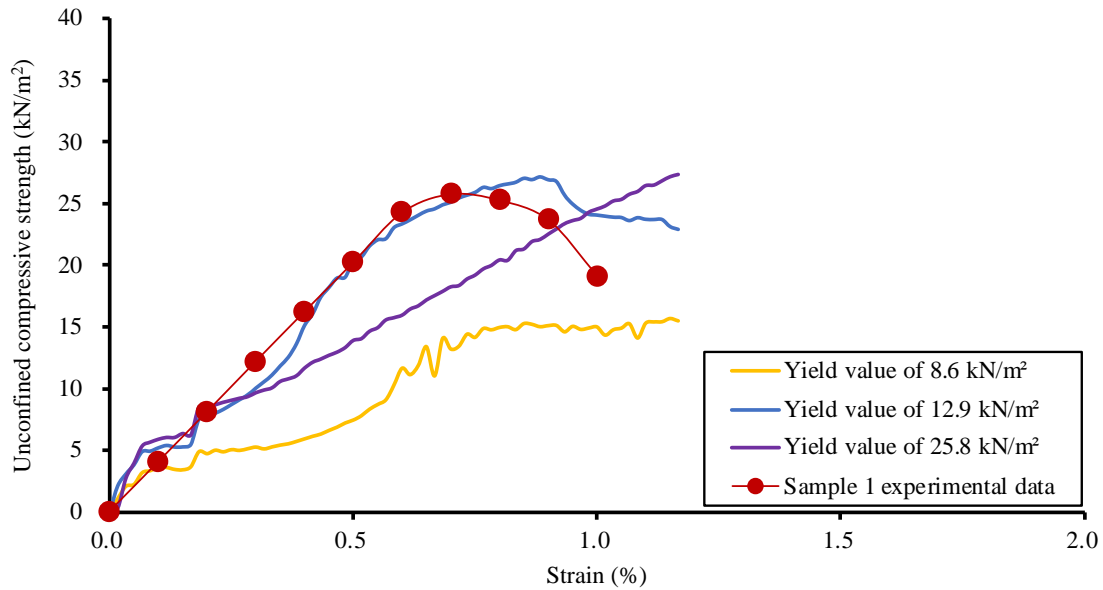


Figure 16. Patterns of sensitivity analysis results for yield values in Sample 1

Table 5. Summary of conditions for sensitivity analysis

Sensitivity analysis	Simulation model	Constant parameter	Varying parameter	Cross Ref.
Plastic viscosity	Sample 1	Yield value = 12.9 kN/m <sup>2</sup> Critical shear strain = 0.000129 s <sup>-1</sup>	Yield parameter is adjusted to change plastic viscosity	Figure 12
	Sample 2	Yield value = 19.743 kN/m <sup>2</sup> Critical shear strain = 0.00012 s <sup>-1</sup>	Yield parameter is adjusted to change plastic viscosity	Figure 13
Critical shear strain	Sample 1	Yield value = 12.9 kN/m <sup>2</sup> Yield parameter = 0.0001	Plastic viscosity is adjusted to change critical shear strain	Figure 14
	Sample 2	Yield value = 19.743 kN/m <sup>2</sup> Plastic viscosity = 13162 Pa·s	Yield parameter is adjusted to change critical shear strain	Figure 15
Yield value	Sample 1	Plastic viscosity = 8600 Pa·s Critical shear strain = 0.00012 s <sup>-1</sup>	Yield parameter is adjusted to change yield value	Figure 16

Table 6. Summary of results for sensitivity analysis relationship

Sensitivity analysis	Other parameters	Theoretical relationship	Influence on simulation results	Cross Ref.
Plastic viscosity	Critical shear strain	Inversely	Highly	Simulation results (Figure 14)
	Yield value	Directly	Slightly	Shakya & Inazumi (2023)
	Yield parameter	Directly	Negligible	Simulation results (Figures 12 and 13)
Critical shear strain	Plastic viscosity	Inversely	Highly	Simulation results (Figure 14)
	Yield value	Directly	Negligible	Deduced from pattern
	Yield parameter	Directly	Slightly	Simulation results (Figure 15)
Yield value	Plastic viscosity	Directly	Slightly	Shakya & Inazumi (2023)
	Critical shear strain	Directly	Negligible	Deduced from pattern
	Yield parameter	Inversely	Highly	Simulation results (Figure 16)
Yield parameter	Plastic viscosity	Directly	Negligible	Simulation results (Figures 12 and 13)
	Critical shear strain	Directly	Slightly	Simulation results (Figure 15)
	Yield value	Inversely	Highly	Simulation results Figure 16)

Although exactly the same stress-strain curve characteristics as those of the target sample soil could not be reproduced in either simulation, the obtained results comprise a guideline for further studies on the determination of the exact material parameter values. Thus, using the previous results as a guideline, the authors attempted to recreate the exact stress-strain relationship for both samples. Figures 17 and 18 provide the stress-strain relationship reproduced for Samples 1 and 2, respectively. It was observed that the strength and strain values were approximately equal in both cases, but that the curve characteristics were not exactly the same at all phases. A graph of the simulation results was plotted for the data consisting of 1-second time intervals, and the formation of minute fluctuations in the curve characteristics could have been avoided for a dataset consisting of longer time intervals.

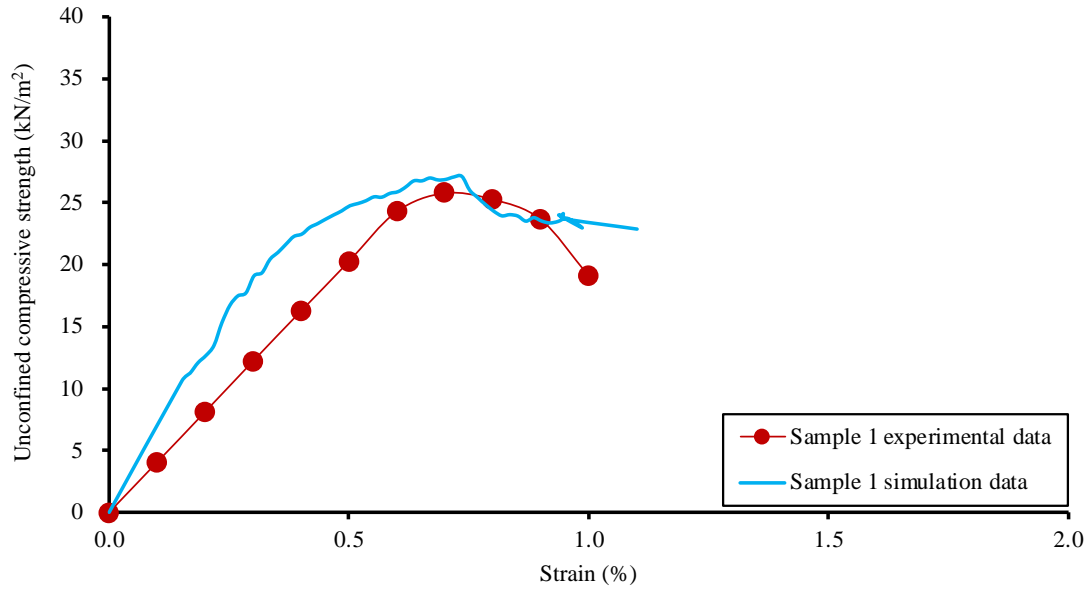


Figure 17. Comparison of experimental and simulation stress-strain curve characteristics for Sample 1

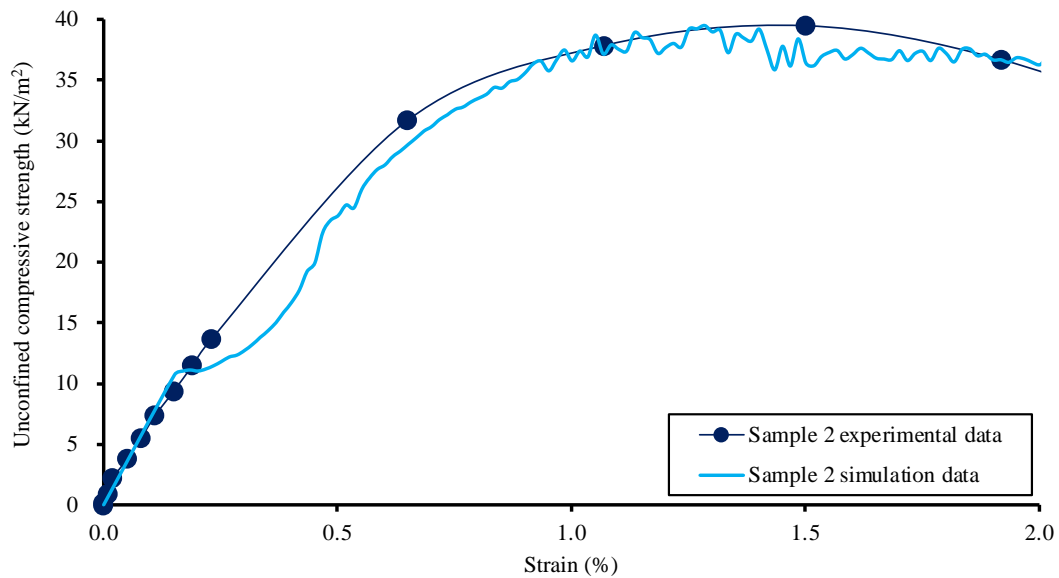


Figure 18. Comparison of experimental and simulation stress-strain curve characteristics for Sample 2

Although this study included a sensitivity analysis of the critical shear strain, the obtained value is not directly inputted during the MPS simulation setting. However, the yield value, plastic viscosity, and yield parameter must be inputted directly, and these parameters are directly related to the critical shear strain, as shown in Equation 6. From this study, it was verified that the critical shear strain should be lower for a higher degree of accuracy and that the value of the yield parameter should also be lower. The theory suggesting that the yield value be equal to half of the unconfined compressive strength has been verified in this study and, considering the relationship between the parameters of the bi-viscosity model, the value for plastic viscosity must also be higher.

## 5. Conclusions

This study was solely focused on the MPS simulation results of unconfined compression tests generated by the different input parameter values. The stress-strain characteristics of two undisturbed soil samples, belonging to the soil and sand categories according to the USDA soil classification, were used as the target values. The results of the study can be divided into two major parts: i) determination of the optimum interparticle distance and initial time interval for the MPS simulation, and ii) sensitivity analysis of the parameters of the bi-viscosity fluid that influences the results. The major conclusions are summarized below.

- Calculations of pressure and viscosity for incompressible fluids by a MPS simulation should be carried out under the implicit method for higher precision.
- Lower values for the interparticle distance generate higher accuracy in the output results. It is desirable to conduct the simulation at an interparticle distance equal to the average dimension of the soil particles. However, it is important to consider the calculation load during the simulation, as lowering the interparticle distance will increase the calculation load.
- The precision of the output results increases with a lower initial interval time value. This value will be treated as the time increment value at which the calculation is carried out. The combination of interparticle distance and initial time increment determines the accuracy and precision of the MPS simulation. Generally, the combination of the interparticle distance of 0.7 mm and the initial time interval of 0.07 s or less will produce output results with satisfactory precision.
- Changing the default value of the radius of influence is generally not recommended. However, in certain simulations, such as those of unconfined compression tests on soil similar to that used in this study, where decreasing the value of the influence radius for surface tension generated slightly better output results, such a change is recommended.
- The parameters under which the sensitivity analysis for plastic viscosity was conducted in this study generated negligible influence. However, it was deduced that the reason for this lies in the change in input value of the yield parameter to maintain the constant critical shear strain. Therefore, it is recommended that the input yield parameter value be set according to the yield value and that the plastic viscosity value be set according to the critical shear strain value.
- It was observed that the accuracy of the simulation increased for lower values of critical shear strain. The critical shear strain value at which the optimum result was obtained is approximately 1/100 times the magnitude of the failure strain value. Thus, as a guideline, it is recommended that the critical shear strain value calculated from the failure strain be input. Considering this research as a case study, the critical strain value for Sample 1 should be around 0.00007 s<sup>-1</sup>, while that for Sample 2 should be around 0.000148 s<sup>-1</sup>.
- As this study verified that the yield value is half of the unconfined compressive strength, it can be used as established knowledge in future studies.

This study was centered on two different samples, which possessed a form and did not flow at the time of the simulation. Therefore, these values are recommended for the solid state of the bi-viscosity model only. The parameter values recommended in this study should only be used for soil samples with equivalent physical and mechanical properties. Moreover, unlike other parameters, the exact value of the plastic viscosity was not determined due to the time constraints of the study. However, guidance has been provided for determining the plastic viscosity value, considering the influencing parameters and the approximate degree of influence. It is suggested that these recommended values be verified if they need to be used for soil samples with different properties.

The samples used in this study were undisturbed samples; thus, Sample 1, despite belonging to the clay category according to the USDA soil classification, had lower unconfined compressive strength. Additional studies might be necessary for reconstituted or compacted clay samples that have higher unconfined compressive strength. Therefore, it will be necessary to verify whether or not the recommended values produce the same degree of precision for these other soil particles. It is expected, however, that the trend of each parameter described in this study will hold true for all soil types, with the exception of a small marginal error depending upon the simulation criteria. As for the precision of the results, despite an attempt to perform the simulation using parameters identical to those of the experimental soil specimens, the presence of unknown factors and the inability to perform the simulation at the actual soil size might have resulted in a slight discrepancy. Moreover, there was a limited calculation capacity, which compelled the analysis conditions to be adjusted such that the number of calculation particles would not exceed the limit that caused the simulation to fail. In conclusion, future studies should be focused on refining the actual parameter values and increasing the database for the different types of soil while considering the limitations of the simulation.

## 6. Declarations

### 6.1. Author Contributions

Conceptualization, S.I.; methodology, S.I.; software, S.I.; validation, S.S. and S.I.; formal analysis, S.S.; investigation, S.S.; resources, S.I.; data curation, S.S.; writing—original draft preparation, S.S.; writing—review and editing, S.I.; visualization, S.S.; supervision, S.I.; project administration, S.I.; funding acquisition, S.I. All authors have read and agreed to the published version of the manuscript.

### 6.2. Data Availability Statement

The data presented in this study are available on request from the corresponding author.

### 6.3. Funding

The authors received no financial support for the research, authorship, and/or publication of this article.

### 6.4. Conflicts of Interest

The authors declare no conflict of interest.

## 7. References

- [1] de Alba, P., & Ballester, T. P. (2006). Residual strength after liquefaction: A rheological approach. *Soil Dynamics and Earthquake Engineering*, 26(2–4), 143–151. doi:10.1016/j.soildyn.2005.02.011.
- [2] Hamada, M., & Wakamatsu, K. (1998). A Study on Ground Displacement Caused By Soil Liquefaction. *Doboku Gakkai Ronbunshu*, 1998(596), 189–208. doi:10.2208/jscej.1998.596\_189.
- [3] Uzuoka, R., Yashima, A., Kawakami, T., & Konrad, J. M. (1998). Fluid dynamics based prediction of liquefaction induced lateral spreading. *Computers and Geotechnics*, 22(3–4), 243–282. doi:10.1016/S0266-352X(98)00006-8.
- [4] Hadush, S., Yashima, A., Uzuoka, R., Moriguchi, S., & Sawada, K. (2001). Liquefaction induced lateral spread analysis using the CIP method. *Computers and Geotechnics*, 28(8), 549–574. doi:10.1016/S0266-352X(01)00016-7.
- [5] Hadush, S., Yashima, A., & Uzuoka, R. (2000). Importance of viscous fluid characteristics in liquefaction induced lateral spreading analysis. *Computers and Geotechnics*, 27(3), 199–224. doi:10.1016/S0266-352X(00)00015-X.
- [6] Yin, D., Zhang, W., Cheng, C., & Li, Y. (2012). Fractional time-dependent Bingham model for muddy clay. *Journal of Non-Newtonian Fluid Mechanics*, 187–188, 32–35. doi:10.1016/j.jnnfm.2012.09.003.
- [7] Chae, J., Kim, B., Park, S. wan, & Kato, S. (2010). Effect of suction on unconfined compressive strength in partly saturated soils. *KSCE Journal of Civil Engineering*, 14(3), 281–290. doi:10.1007/s12205-010-0281-7.
- [8] Kato, S., Yoshimura, Y., Kawai, K., & Sunden, W. (2001). Effects of Suction on Strength Characteristics of Unconfined Compression Test for a Compacted Silty Clay. *Doboku Gakkai Ronbunshu*, 2001(687), 201–218. doi:10.2208/jscej.2001.687\_201.
- [9] Geertsema, M., Hungr, O., Schwab, J. W., & Evans, S. G. (2006). A large rockslide - Debris avalanche in cohesive soil at Pink Mountain, northeastern British Columbia, Canada. *Engineering Geology*, 83(1–3), 64–75. doi:10.1016/j.enggeo.2005.06.025.
- [10] Luna, B. Q., Remaître, A., van Asch, T. W. J., Malet, J. P., & van Westen, C. J. (2012). Analysis of debris flow behavior with a one dimensional run-out model incorporating entrainment. *Engineering Geology*, 128, 63–75. doi:10.1016/j.enggeo.2011.04.007.
- [11] Marr, J. G., Elverhø, A., Harbitz, C., Imran, J., & Harff, P. (2002). Numerical simulation of mud-rich subaqueous debris flows on the glacially active margins of the Svalbard-Barents Sea. *Marine Geology*, 188(3–4), 351–364. doi:10.1016/S0025-3227(02)00310-9.
- [12] Montassar, S., & de Buhan, P. (2006). A numerical model to investigate the effects of propagating liquefied soils on structures. *Computers and Geotechnics*, 33(2), 108–120. doi:10.1016/j.compgeo.2006.02.003.
- [13] Wachs, A. (2007). Numerical simulation of steady Bingham flow through an eccentric annular cross-section by distributed Lagrange multiplier/fictitious domain and augmented Lagrangian methods. *Journal of Non-Newtonian Fluid Mechanics*, 142(1–3), 183–198. doi:10.1016/j.jnnfm.2006.08.009.
- [14] Shakya, S., & Inazumi, S. (2023). Ground modelling by MPS-CAE simulation under different influencing parameters. *Smart Geotechnics for Smart Societies*, 2365–2369. doi:10.1201/9781003299127-365.
- [15] Aberqi, A., Aboussi, W., Benkhaldoun, F., Bennouna, J., & Bradji, A. (2023). Homogeneous incompressible Bingham viscoplastic as a limit of bi-viscosity fluids. *Journal of Elliptic and Parabolic Equations*, 9(2), 705–724. doi:10.1007/s41808-023-00221-z.

- [16] Iribe, T., Iriha, S., Tomiyama, J. and Matsubara, H., (2003). Application of particle method to flow analysis of fresh concrete. *Proceedings of the Japan Concrete Institute*, 25(1), 905-910.
- [17] Urano, S., Nemoto, H., & Sakihara, K. (2012). Application of flow simulation for evaluation of filling-ability of self-compacting concrete. *Journal of Japan Society of Civil Engineers, Ser. E2 (Materials and Concrete Structures)*, 68(1), 38-48. doi:10.2208/jscejmcs.68.38.
- [18] Inazumi, S., Shakya, S., Komaki, T., & Nakanishi, Y. (2021). Numerical analysis on performance of the middle-pressure jet grouting method for ground improvement. *Geosciences (Switzerland)*, 11(8), 313. doi:10.3390/geosciences11080313.
- [19] Shakya, S., Inazumi, S., & Nontananandh, S. (2022). Potential of Computer-Aided Engineering in the Design of Ground-Improvement Technologies. *Applied Sciences (Switzerland)*, 12(19), 9675. doi:10.3390/app12199675.
- [20] Garrido, L., Gainza, J., & Pereira, E. (1988). Influence of sodium silicate on the rheological behaviour of clay suspensions- Application of the ternary Bingham model. *Applied Clay Science*, 3(4), 323-335. doi:10.1016/0169-1317(88)90023-3.
- [21] Leonardi, C. R., Owen, D. R. J., & Feng, Y. T. (2011). Numerical rheometry of bulk materials using a power law fluid and the lattice Boltzmann method. *Journal of Non-Newtonian Fluid Mechanics*, 166(12-13), 628-638. doi:10.1016/j.jnnfm.2011.02.011.
- [22] Aierken, A., Luo, S., Jiang, J., Chong, L., Chang, J., Zhang, R., & Zhang, X. (2022). Experimental and Numerical Studies on Flowing Properties of Grouting Mortar Based on the Modified MPS Method. *Geofluids*, 2022. doi:10.1155/2022/4042418.
- [23] Shakya, S., Inazumi, S., Chao, K. C., & Wong, R. K. N. (2023). Innovative Design Method of Jet Grouting Systems for Sustainable Ground Improvements. *Sustainability*, 15(6), 5602. doi:10.3390/su15065602.
- [24] Hossain, M. S., & Kim, W. S. (2015). Estimation of Subgrade Resilient Modulus for Fine-Grained Soil from Unconfined Compression Test. *Transportation Research Record*, 2473(1), 126-135. doi:10.3141/2473-15.
- [25] Güneşli, H., & Rüşen, T. (2016). Effect of length-to-diameter ratio on the unconfined compressive strength of cohesive soil specimens. *Bulletin of Engineering Geology and the Environment*, 75(2), 793-806. doi:10.1007/s10064-015-0835-5.
- [26] Shakya, S., & Inazumi, S. (2023). Soil Behavior Modeling By MPS-CAE Simulation. *International Journal of GEOMATE*, 24(102), 18-25. doi:10.21660/2023.102.g12141.
- [27] Inazumi, S., Kuwahara, S., Ogura, T., Hamada, S., & Nakao, K. (2020). Visualization and performance evaluation of existing pile pulling method with pile tip chucking by MPS-CAE. *Japanese Geotechnical Journal*, 15(2), 383-393. doi:10.3208/jgs.15.383.
- [28] Kondo, M., & Koshizuka, S. (2008). Suppressing the Numerical Oscillations in Moving Particle Semi-implicit method. *Transactions of the Japan Society for Computational Engineering and Science*, 20080015, 20080015. doi:10.11421/jscses.2008.20080015.
- [29] Koshizuka, S., & Oka, Y. (1996). Moving-particle semi-implicit method for fragmentation of incompressible fluid. *Nuclear Science and Engineering*, 123(3), 421-434. doi:10.13182/NSE96-A24205.
- [30] Cummins, S. J., & Rudman, M. (1999). An SPH Projection Method. *Journal of Computational Physics*, 152(2), 584-607. doi:10.1006/jcph.1999.6246.
- [31] Jandaghian, M., & Shakibaeinia, A. (2020). An enhanced weakly-compressible MPS method for free-surface flows. *Computer Methods in Applied Mechanics and Engineering*, 360, 112771. doi:10.1016/j.cma.2019.112771.
- [32] Shakibaeinia, A., & Jin, Y. C. (2010). A weakly compressible MPS method for modeling of open-boundary free-surface flow. *International Journal for Numerical Methods in Fluids*, 63(10), 1208-1232. doi:10.1002/flid.2132.
- [33] Tayebi, A., & Jin, Y. chung. (2015). Development of Moving Particle Explicit (MPE) method for incompressible flows. *Computers and Fluids*, 117, 1-10. doi:10.1016/j.compfluid.2015.04.025.
- [34] Kodama, Y. (2008). Explicit and Implicit Methods. *Computational Fluid Dynamics*, 687, 416-417. doi:10.1016/b978-075068563-4.50013-6.
- [35] Hu, F., Xu, C., Li, H., Li, S., Yu, Z., Li, Y., & He, X. (2015). Particles interaction forces and their effects on soil aggregates breakdown. *Soil and Tillage Research*, 147, 1-9. doi:10.1016/j.still.2014.11.006.
- [36] Itori, S., Iribe, T., & Nakaza, E. (2012). An Improvement of Dirichlet Boundary Conditions in Numerical Simulations Using MPS Method. *Journal of Japan Society of Civil Engineers, Ser. B2 (Coastal Engineering)*, 68(1), 17-28. doi:10.2208/kaigan.68.17.